

Repetitive control of CATOFIN process

Seung-Taek Seo, Wangyun Won*, Kwang Soon Lee*,†, Chansul Jung** and Seokho Lee**

Honeywell Co. Ltd., Seoul 140-702, Korea

*Department of Chemical and Biomolecular Engineering, Sogang University,
Shinsoodong-1, Mapogu, Seoul 121-742, Korea

**Samsung Engineering Co. Ltd., Seoul 135-854, Korea
(Received 1 November 2006 • accepted 30 March 2007)

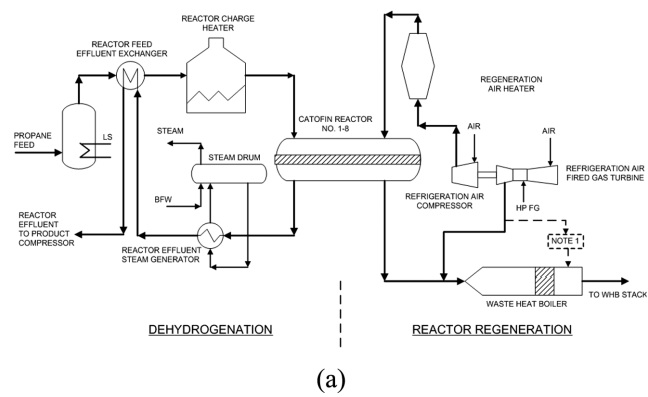
Abstract—The CATOFIN process is a propane dehydrogenation process for production of propylene. It uses multiple adiabatic fixed-bed reactors where dehydrogenation and regeneration (decoking) are performed alternatively over roughly ten minutes of period for each operation. Taking advantage of the periodic operation, the present research concerns the development of a repetitive control method to improve the operation of the CATOFIN process. The controller is designed to perform feedback action during the regeneration cycle and to perform only state estimation during the dehydrogenation cycle. To improve the performance while overcoming the nonlinearity of the process, a linearized time-varying process was derived from a first-principle model and used for the controller design.

Key words: CATOFIN Process, Repetitive Control, Fixed-bed Reactor

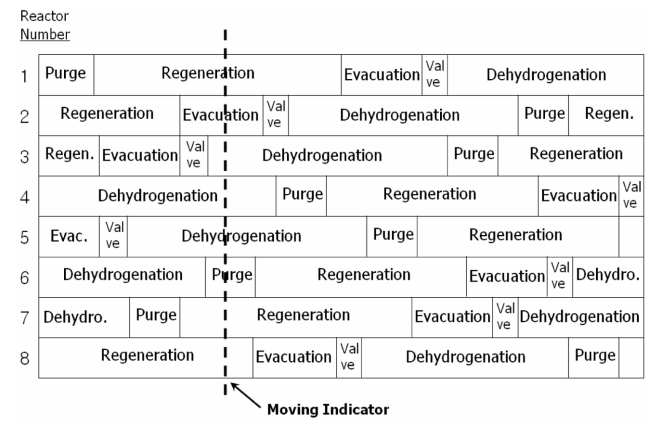
INTRODUCTION

Ethylene and propylene, the basic precursor feedstocks in the petrochemical industry, have been mainly produced by thermal cracking of naphtha, ethane and propane. Recently, the CATOFIN process has emerged as a competitive propylene production process due to its higher product selectivity, energy efficiency, and low operating cost with the advance of the catalyst [1]. The CATOFIN process consists of multiple parallel adiabatic fixed-bed reactors, where dehydrogenation (Dehyd) of propane and catalyst regeneration (Regen) by decoking are carried out alternatively over roughly ten minutes of period for each operation. During the Dehyd operation, bed temperature is gradually decreased by the endothermic reaction. Then the bed temperature is restored to the original state during the exothermic Regen period. By exquisite scheduling of the multiple reactor beds, Dehyd incessantly takes place in a same number of reactors so that propylene production can be continuous. Fig. 1 shows a process flow diagram of the CATOFIN process. However, optimal operation of the reactors in the CATOFIN process is a tricky issue because of complex dynamics caused by the unsteady operation and inherent nonlinearity.

There have been a large number of studies on propane Dehyd and catalyst Regen from reaction kinetics to reactor dynamics and control. The references in [2-8] are only a part of them. However, the CATOFIN process is relatively new and the dynamics and control studies on the concerned reactor seem to be rare in the open literature according to the authors' survey. In the industrial CATOFIN process, the main concern is to maintain the reactor operation at the optimum condition overcoming the gradual catalyst deactivation. This is a combined problem of optimization, on-line model identification, and control. The major mission of the controller is to steer the reactor to new set points dictated by the optimizer. Hence



(a)



(b)

Fig. 1. Process flow diagram of the CATOFIN process.

the set point tracking is the major task of the controller in the CATOFIN process.

The reactors in the CATOFIN process are under repetitive (or cyclic) operation where the results of a previous run affect the operation of the upcoming runs. In a loose sense, however, the reactors

*To whom correspondence should be addressed.

E-mail: kslee@sogang.ac.kr

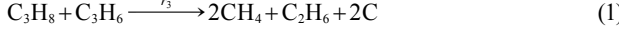
can be said to undergo batch operation since some resetting operations are inserted between Dehyd and Regen cycles. It is obvious that an advanced industrial control technique like MPC (Model Predictive Control) is not adequate for the CATOFIN reactor since the process is not under a steady state operation.

In this research, a repetitive control (RC) method has been developed for CATOFIN reactor operation as one of the essential modules of an on-line optimization system of the CATOFIN process. The RC method is a special control technique for repetitive processes [9,10]. It can perform not only real-time feedback control but also cycle-wise information feedback. Due to the latter action, it can achieve perfect tracking, overcoming cycle-wise repeated disturbances and model error. The RC method proposed in this research is based on the model obtained by linearization of a first-principle model around the operating trajectories in the previous cycle. The repetitive controller was devised to regulate the bed temperatures measured at two axial positions on desired values at the end of each Regen cycle. The flow rate and temperature of the feed air for the Regen cycle were chosen as the manipulated variables (MV's).

PROCESS DESCRIPTION

1. Reactions and Reactor Operation

Eqs. (1) and (2) show the dominant reactions taking place during Dehyd and Regen, respectively [6].



During Dehyd, all the manipulated variables are kept at pre-specified constant values for consistent propylene production. During Regen,

however, both flow rate and temperature of the combustion air are manipulated to steer the bed temperatures to desired values overcoming possible disturbance effects.

It is assumed that both Dehyd and Regen last for nine minutes each and real-time measurements are available only for bed temperatures at four discrete axial positions, $z=0.2, 0.4, 0.6$, and 0.8 .

2. Mass and Energy Balances

It is assumed that the concentration and temperature in the reactor have no distribution along the radial direction. Under this condition, the component mass balance is written by neglecting the radial and also axial dispersion terms as

$$\begin{aligned} \frac{\partial C_i}{\partial t} &= -\left(\frac{v_g}{L}\right)\frac{\partial C_i}{\partial z} + \left(\frac{1-\varepsilon}{\varepsilon}\right)\rho_c \bar{r}_i \\ \frac{\partial C_c}{\partial t} &= \rho_c \bar{r}_c \\ \text{I.C.: } C_i &= C'_i(z) \quad \text{at } t=0 \\ \text{B.C.: } C_i &= C^0_i(t) \quad \text{at } z=0 \end{aligned} \quad (3)$$

where L , v_g , ε , and ρ_c denote bed length, linear gas velocity (m/min), bed porosity, and catalyst density (kg/m^3), respectively; \bar{r}_i and C_i represent the rate of generation ($\text{kmol}/\text{kg}\cdot\text{cat}\cdot\text{min}$) and concentration (kmol/m^3) of component i . The second equation in Eq. (3) is for carbon which is deposited on the catalyst surface where it is generated.

The energy balance is given by

$$\begin{aligned} \frac{\partial T}{\partial t} &= -\left(\frac{\varepsilon}{1-\varepsilon}\right)\left(\frac{\rho_g c_{pg} v_g}{\rho_c c_{pc} L}\right)\frac{\partial T}{\partial z} + \left(\frac{k_B}{\rho_c c_{pc} L^2}\right)\frac{\partial^2 T}{\partial z^2} - \left(\frac{1}{c_{pc}}\right)\sum_j \Delta H_j r_j \\ \text{I.C.: } T &= T_o(z) \quad \text{at } t=0 \\ \text{B.C.: } T &= T_o \quad \text{at } z=0, \frac{dT}{dz}=0 \quad \text{at } z=1 \end{aligned} \quad (4)$$

where ρ_g , c_{pg} , and c_{pc} are gas density (kg/m^3), specific heats ($\text{kcal}/\text{kg}\cdot\text{K}$) of gas and catalyst, respectively; k_B denotes thermal conductivity ($\text{kcal}/\text{min}\cdot\text{m}\cdot\text{K}$) of the catalyst bed; r_j and ΔH_j represent the reaction rate for the j^{th} reaction path and the corresponding heat of

Table 1. Simulation conditions and parameters

Process	Parameters			
Reactor size	Length=1.1152 m			
Conditions	Inlet temp.=650 °C, Reactor temp.=650 °C Propane flow=2,500 kg/min $\rho_g=0.291 \text{ kg}/\text{m}^3$, $v_g=84.8 \text{ m}/\text{min}$ $k_B=0.472 \text{ kcal}/\text{min}\cdot\text{m}\cdot\text{K}$ $C_g (\text{kcal}/\text{kg}\cdot\text{K})=(\bar{R}/M)[1.213+28.785*10^{-3}T-8.824*10^6T^2]$ $C_c (\text{kcal}/\text{kg}\cdot\text{K})=0.0015754 [227.25-0.02132T+3543029T^2-2567.3T^{0.5}]$ $P=0.5 \text{ atm}$			
Dehydrogenation	Reaction	r_1	$k_1 [\text{C}_3\text{H}_8]\text{RT}$	
		r'_1	$k'_1 [\text{C}_3\text{H}_8][\text{H}_2]\text{R}^2\text{T}^2$	
		r_2	$k_2 [\text{C}_3\text{H}_6]\text{R}^2\text{T}^2$	
		r_3	$k_3 [\text{C}_3\text{H}_8][\text{C}_3\text{H}_6]\text{R}^2\text{T}^2$	
Regeneration	Conditions	Inlet temp.=690 °C Air flow=180 ton/h $\rho_g=0.725 \text{ kg}/\text{m}^3$, $v_g=45.2 \text{ m}/\text{min}$		
		Reaction		
		r_4	$k_4[\text{C}][\text{O}_2]\text{RT}$	
			$k_4: 10^5 \exp(-107000/8.314T)$	

$$R=0.08206 (\text{atm m}^3/\text{kmol K}), \bar{R}=1.9872 (\text{cal/mol K})$$

reaction (kcal/kmol). The parameters for mass and energy balances were taken from the works by Mickley et al. [7] and Kim et al. [8].

Dehyd and Regen models are obtained separately with the associated partial differential equations and then reduced to sets of ordinary differential equations (ODE) using the cubic spline collocation method [11,12] with six equally spaced collocation points including $z=0$ and 1. In the above modeling, the effects of preparative operations like purge and evacuation, which were resetting opera-

tions between Dehyd and Regen cycles, were not considered assuming that the switching between Dehyd and Regen operations is made seamlessly.

Table 1 shows the reactor parameters and normal operating conditions. In practice, the active sites on the catalyst surface are reduced by coking during Dehyd, which causes a gradual change in the reaction rate. In the present study, however, this change was not considered in the reactor model.

3. Process Simulation

Fig. 2 shows the time-dependent trajectories of the bed temperatures at six axial positions during Dehyd and Regen cycles, respectively, after they reach a periodic steady state. By the endothermic reactions, bed temperatures are decreased as propane Dehyd proceeds, but restored by the heat of combustion during the decoking operation.

Fig. 3 shows the corresponding trajectories of propane and propylene concentrations. If we closely compare Figs. 2 and 3, it can be recognized that the front half of the bed where temperatures are higher than the rear half contributes the most part of the propylene production.

In Fig. 4, trajectories for coke deposit at different axial positions are shown under a periodic steady state. During the Dehyd cycle, elementary carbon is produced according to Eq. (1) and deposited on the catalyst surface. In the regeneration cycle, hot air is injected and burns the deposited carbon resulting in a rise of bed temperature.

CONTROLLER DESIGN

1. Discretized Model

For controller design, the ODE reactor models for Dehyd and Regen were discretized along the time domain through forward difference approximation. For the k^{th} -cycle, the resulting model can be written as

$$\begin{aligned} x_k(t+1) &= g(x_k(t), u_k(t)) \\ y_k(t) &= Cx_k(t) \end{aligned} \quad (5)$$

with

$$\begin{aligned} g &= \begin{cases} g^D & \text{for } t \in [0, t_{deh}] \\ g^R & \text{for } t \in [t_{deh} + 1, N] \end{cases} \\ (x, u) &= \begin{cases} (x^D, 0) & \text{for } t \in [0, t_{deh}] \\ (x^R, [T_{air} q_{air}]) & \text{for } t \in [t_{deh} + 1, N] \end{cases} \end{aligned} \quad (6)$$

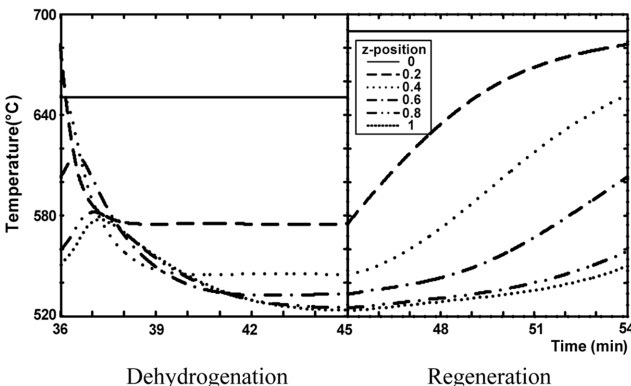


Fig. 2. Bed temperature trajectories at six axial positions under a periodic steady state.

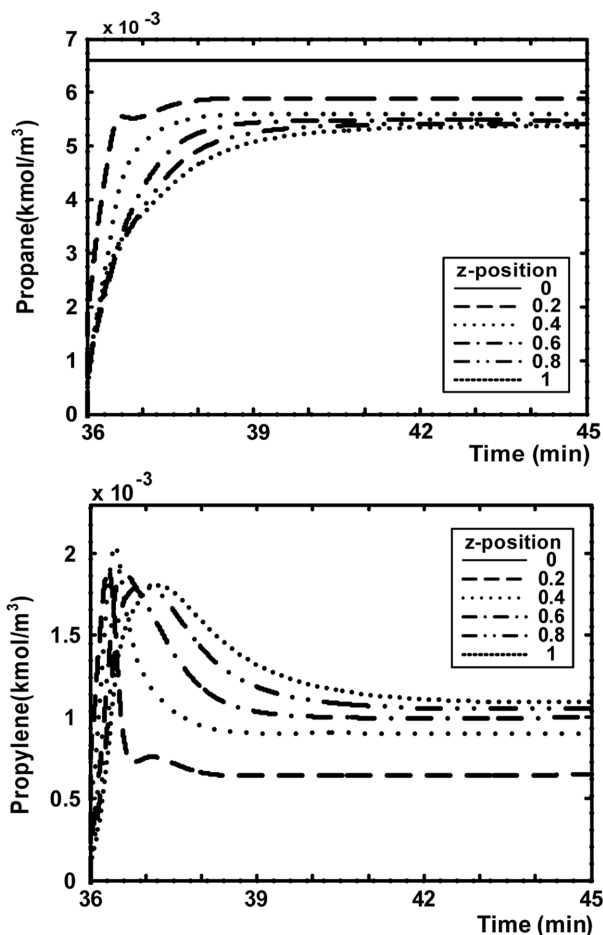


Fig. 3. Trajectories of propane and propylene concentrations at six axial positions under a periodic steady state.

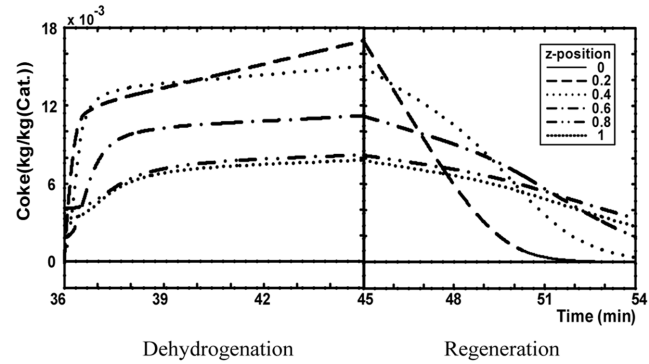


Fig. 4. Trajectories of coke deposit at six axial positions under a periodic steady state.

under the assumption that one cycle begins with Dehyd operation, where the superscripts ^D and ^R represent the variables associated with the Dehyd and Regen modes, respectively; t_{deh} and N denote the terminal times of Dehyd and Regen operations, respectively; x represents the state which consists of the concentrations of the associated components and the bed temperatures at the collocation points; y denotes the measured output, the bed temperatures at four axial positions; and u represents the manipulated variable (MV), which is void for Dehyd, but represents the temperature and flow rate of the combustion air for Regen. The states are switched according to

$$x_k^R(t_{deh}+1) = Mx_k^D(t_{deh}) \text{ and } x_{k+1}^D(1) = Px_k^R(t_{deh}) \quad (7)$$

where M is a matrix that transfers the part of $x_k^D(t_{deh})$ corresponding to the bed temperature and coke deposit to $x_k^R(t_{deh})$ and resets the remaining part of $x_k^R(t_{deh})$ that corresponds to the initial oxygen concentrations to zero. P is defined in a similar way.

During the Dehyd cycle, there is no control action and only the state estimation is carried out. In this case, the extended Kalman filter can be employed for Eq. (5). During the Regen cycle, the control action needs to be determined. To include the cycle-wise integral action in the controller while reflecting the nonlinear traits of the reactor as much as possible, Eq. (5) was linearized around the time-dependent input, state, and output trajectories obtained in the previous cycle. Then we have

$$\begin{aligned} \Delta x_k(t+1) &= A_{k-1}(t)\Delta x_k(t) + B_{k-1}(t)\Delta u_k(t) \\ y_k(t) &= y_{k-1}(t) + C\Delta x_k(t) \end{aligned} \quad (8)$$

where $\Delta x_k(t)@x_k(t)-x_{k-1}(t)$, $\Delta u_k(t)@u_k(t)-u_{k-1}(t)$; $A_{k-1}(t)$ represents a shorthand notation of $A(u_{k-1}(t), x_{k-1}(t))$, and similarly for $B_{k-1}(t)$.

2. Control Algorithm

The control objective has been placed in the regulation of bed temperatures at two axial positions at the end of the Regen operation at desired values. These temperatures are denoted $\bar{y}_k(N-1)$ as in this paper. For such end point control, manipulation of $u_k(t)$ at every sampling instant is not necessary. In this research, $u_k(t)$ is constrained to change only three times during the Regen operation at $t_1=t_{deh}+1$, t_2 , and $t_3 < N-1$. Under this restriction, the controller is designed to perform the following step-by-step actions during an entire cycle:

[Step 1] State estimation during the Dehyd operation:

Using the extended Kalman filter (EKF) applied to Eq. (5), $x_k^D(t)$ is estimated over $[1, t_{deh}]$ using the bed temperature measurements.

[Step 2] State transition from the Dehyd to Regen operations:

Using the EKF estimates $x_k^D(t_{deh}|t_{deh})$, $x_{k-1}^D(t_{deh}|t_{deh})$, and the state transition rule in Eq. (7), the initial value $\Delta x_k^D(t_{deh}+1|t_{deh})$ for the Kalman filter for the Regen operation is given. Here, $x(t|\tau)$ represents an optimal estimate of $x(t)$ based on the information up to τ .

[Step 3] Calculation of the first control action in the Regen operation:

For simplicity, let $t_1@t_{deh}+1$ and $\Delta x_k@x_k^D$. At t_1 , $\bar{y}_k(N-1|t_1)$, an optimal prediction of $\bar{y}_k(N-1)$ based on the information at t_1 , is obtained as a function of $\Delta u_k(t_i)$, $i=1, 2, 3$, and the state estimate $\Delta x_k(t_i|t_1)$. The input changes are determined such that

$$\min_{\Delta u_k(t)} \left[\|r - \bar{y}_k(N-1|t_1)\|_Q^2 + \sum_{i=1}^3 \|\Delta u_k(t_i)\|_R^2 \right] \quad (9)$$

subject to other constraints

$u_k(t_i) = u_{k-1}(t_i) + \Delta u_k(t_i)$ is applied to the process.

[Step 4] State estimation in the Regen operation:

Between t_1 and t_2 , only state estimation is performed by using the Kalman filter applied to Eq. (8) while maintaining the MV at $u_k(t_1)$.

[Step 5] Repeat steps 3 and 4:

Repeat steps 3 and 4 for t_2 and also for t_3 .

[Step 6] Transition to next cycle:

Using Eq. (7), $\Delta x_{k+1}^D(1|0)$ is obtained from $\Delta x_k^R(N|N)$. From this, $x_{k+1}^D(1|0)$ is calculated by adding $x_k^D(1|0)$.

The EKF equation for the Dehyd operation applied to Eq. (5) looks like

$$\begin{aligned} x_k(t+1|t) &= g(x_k(t|t)) \\ x_k(t|t) &= x_k(t|t-1) - K^D(t)(y_k(t) - C_x(t|t-1)) \end{aligned} \quad (10)$$

Also, the Kalman filter for the Regen operation applied to Eq. (8) is described as

$$\begin{aligned} \Delta x_k(t+1|t) &= A_{k-1}(t)\Delta x_k(t|t) + B_{k-1}(t)\Delta u_k(t) \\ \Delta x_k(t|t) &= \Delta x_k(t|t-1) - K^R(t)(y_k(t) - y_{k-1}(t) - C(t)\Delta x_k(t|t-1)) \end{aligned} \quad (11)$$

In the above, the formulas for the time-varying Kalman gains K^D and K^R can be found in standard textbooks. See [13] for example. The covariance matrices for the process and measurement noises needed in the computation of the Kalman gains can be considered as tuning factors and can be adjusted according to the model accuracy and measurement reliability. In Eq. (11), $y_{k-1}(t)$ needs to be replaced by $y_{k-1}(t|t)$ or other more rigorous estimate. For more details on this issue, see [8].

The optimal prediction $\bar{y}_k(N-1|t_1)$ is given by the following equation:

$$\begin{aligned} \bar{y}_k(N-1|t_1) &= \bar{y}_{k-1}(N-1|N-1) + \Pi(t_1)\Delta x_k(t_1|t_1) \\ &\quad + G_1(t_1)\Delta u_k(t_1) + G_2(t_1)\Delta u_k(t_2) + G_3(t_1)\Delta u_k(t_3) \end{aligned} \quad (12)$$

where

$$\begin{aligned} \Pi(t_1) @ \bar{C}A(N-2)L & A(t_1) \\ G_1(t_1) @ \bar{C}A(t_2-2)L & A(t_1+1)B(t_1) + L + \bar{C}B(t_2-2) \\ G_2(t_1) @ \bar{C}A(t_3-2)L & A(t_2+1)B(t_2) + L + \bar{C}B(t_3-2) \\ G_3(t_1) @ \bar{C}A(N-2)L & A(t_3+1)B(t_3) + L + \bar{C}B(t_3-2) \end{aligned}$$

In the above, \bar{C} is the output matrix for $\bar{y}_k(t)$; matrices Π, L, G_3 are dependent on k but the dependency is not explicitly expressed for simplicity. The output predictions $\bar{y}_k(N-1|t_2)$ and $\bar{y}_k(N-1|t_3)$ are given similarly to Eq. (12).

3. Controller Implementation

The sampling period was chosen to be 3 sec, resulting in total sampling instants of $N=360$ over an entire cycle. Hence, each of the Dehyd and Regen operations has 180 sampling instants. The control moments, t_1 , t_2 , and t_3 , were chosen as 181, 240, and 300, respectively. The controlled variable $\bar{y}_k(t)$ was chosen as the bed temperature at $z=0.2$ and 0.4, respectively. The weighting matrices were tuned such that the ratio of the sum of squared output error to the sum of input change in Eq. (9) is approximately 1 : 0.2.

The following constraints were imposed on the MV movements:

$$\begin{aligned} 150 \leq q_{air}(\text{air flow rate}) &\leq 181(\text{ton/h}) \\ 660 \leq T_{air}(\text{air temperature}) &\leq 720(\text{°C}) \end{aligned} \quad (13)$$

The above are typical values from a commercial plant producing

455,000 (ton/yr) [14].

RESULTS AND DISCUSSION

Performance of the controller has been investigated for two cases of set point changes. In the first case, the set point was changed from [681.9 °C 651.6 °C], which is the output values under the cyclic steady state with $[q_{air} T_{air}] = [180 \text{ ton/h } 690 \text{ °C}]$, to [690 °C 655 °C]. In the

second case, the set point change was given from [681.9 °C 651.6 °C] to [690 °C 660 °C]. Also, to demonstrate the performance to achieve zero offset overcoming the model uncertainty, random errors of maximum 10% were imposed on the parameters for the reaction rates in the nominal reactor model for controller design. In the above, it is noted that the normal air flow rate is given to be very close to the compressor capacity limit. It is a frequently encountered industrial situation due to the high equipment price of compressors.

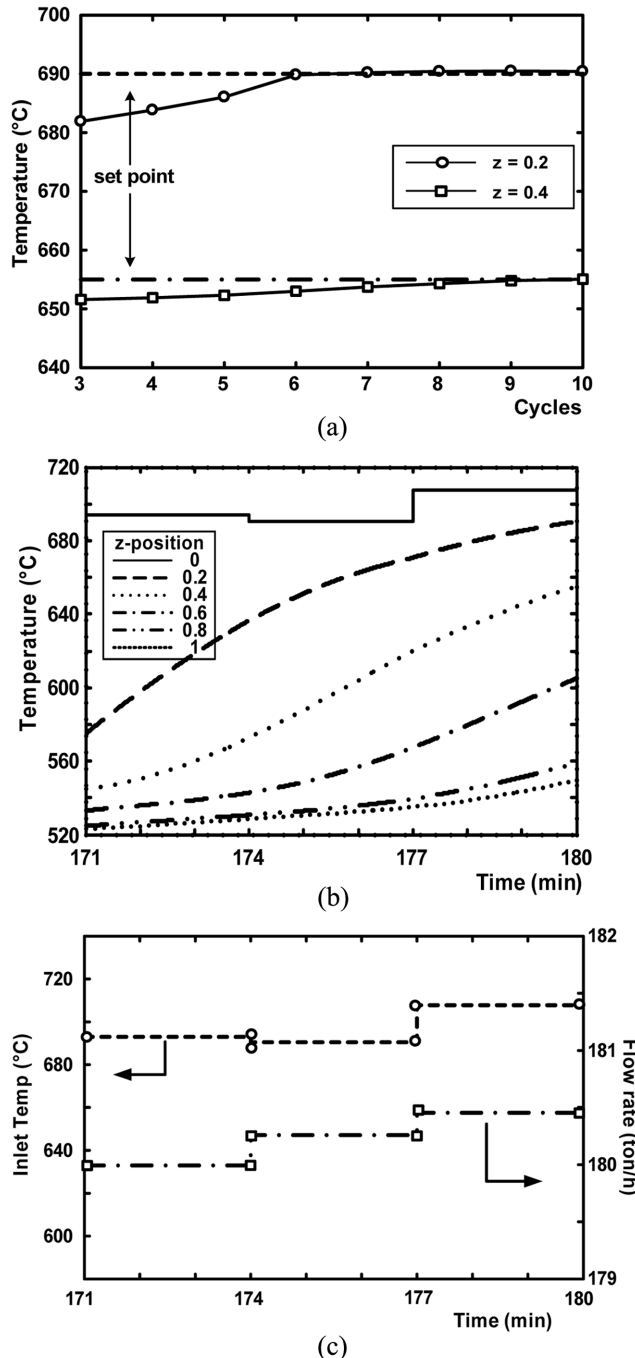


Fig. 5. Results of repetitive control for a set point change to [690 °C 655 °C]: (a) two controlled bed temperatures during the Regen operation, (b) and (c) bed temperature and input profiles, respectively, after the cyclic steady state is reached.

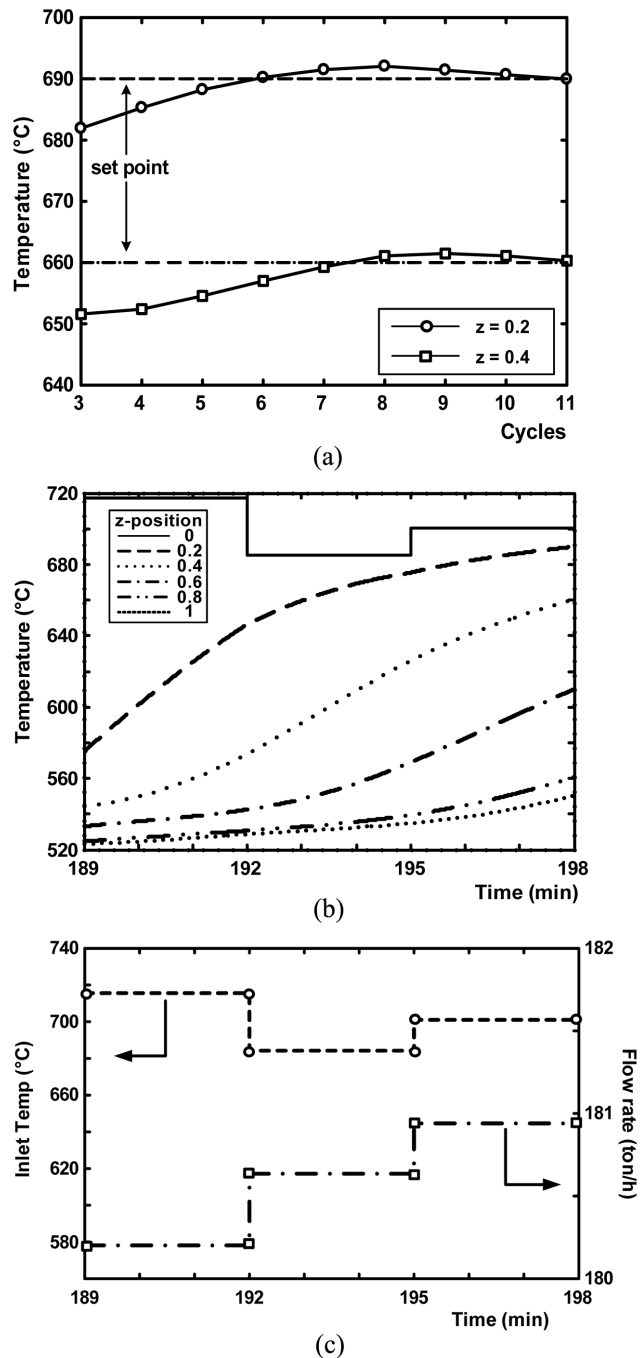


Fig. 6. Results of repetitive control for a set point change to [690 °C 660 °C]: (a) two controlled bed temperatures during the Regen operation, (b) and (c) bed temperature and input profiles, respectively, after the cyclic steady state is reached.

In Fig. 5, the response of the bed temperatures at $z=0.2, 0.4$ and input changes to the first set point change are shown. Fig. 5(a) represents the two controlled bed temperatures at the terminal time of Regen operations. It can be observed that the outputs settle on the respective set points in around nine cycles. Figs. 5(b) and 5(c) show the bed temperature and input profiles, respectively, after the cyclic steady state is reached.

In Fig. 6, output responses to the second set point change are shown. In this case, compared to the first set point change, only the second bed temperature (at $z=0.4$) is forced to increase by 5°C more. In this case, the bed temperatures are subject to some overshoot but settle in around 11 cycles of operation. The resulting transient periods are only typical ones and they can be shortened or lengthened by the weighting matrices in the quadratic objectives and also the covariance matrices for the Kalman filter.

CONCLUSIONS

Through this study, a model-based repetitive controller has been proposed and applied to a numerical CATOFIN process in the course of developing an on-line optimizer for the CATOFIN process, where optimizing the reactor operating conditions overcoming catalyst deactivation is important. It was assumed that the bed temperatures are controlled by manipulating the flow rate and temperature of combustion air for decoking. A repetitive control algorithm has been devised to minimize a quadratic error criterion using a physical model of the CATOFIN process. Thanks to the period-wise feedback, the proposed controller showed quite satisfactory performance against set point changes and model uncertainty.

ACKNOWLEDGMENTS

This work was supported by grant No. 2005-E-ID03-P-02-0-000

from Korea Research Foundation program of the Korea Energy Management Corporation.

REFERENCES

1. [http://www02.abb.com/GLOBAL/NOOFS/noofs187.nsf/viewunid/E737E35CA38F5161C12569EE0036977D/\\$file/CATOFIN.pdf](http://www02.abb.com/GLOBAL/NOOFS/noofs187.nsf/viewunid/E737E35CA38F5161C12569EE0036977D/$file/CATOFIN.pdf)
2. J. A. Pena, A. Monzon and J. Santamaria, *Applied Catalysis A*, **101**, 185 (1993).
3. D. O. Borio and N. S. Schbib, *Comp. Chem. Eng.*, **19**, Suppl., 345 (1995).
4. A. Brito, R. Arvelo, F. J. Garcia and A. R. Gonzalez, *Applied Catalysis A*, **145**, 285 (1996).
5. J. Gascon, C. Tellez, J. Herguido and M. Menendez, *Applied Catalysis A*, **248**, 105 (2003).
6. C. Kern and A. Jess, *Chem. Eng. Sci.*, **60**, 4249 (2005).
7. H. S. Mickley, J. W. Nestor, Jr. and L. A. Gould, *The Can. J. Chem. Eng.*, 61 (1965).
8. Y. G Kim, H. S. Lee and Y. S. Song, *Korean J. Chem. Eng.*, **18**, 11 (1980).
9. J. H. Lee, S. Natarajan and K. S. Lee, *J. Process Control*, **11**, 195 (2001).
10. S. Hara, Y. Yamamoto, T. Omata and N. Nakano, *IEEE Trans. AC*, **33**, 659 (1988).
11. S. Y. Choi, H. S. Kim, K. S. Lee, K. P. Yoo and W. H. Lee, *Korean J. Chem. Eng.*, **8**, 44 (1991).
12. W. H. Yun and K. S. Lee, to be published in *Korean J. Chem. Eng.*.
13. K. J. Åström and B. Wittenmark, *Computer controlled systems*, 3rd ed., Prentice Hall, New York, NY (1997).
14. Private communication with process engineers in Samsung Engineering Co., Korea.